



Mechanical response analysis of buried natural gas pipelines due to excavation unloading

YUKUN LI¹, PENG ZHOU^{1,*}, SHANGXIN ZHAO², CHENLIANG PEI¹, AO YANG¹ and ZIXIU ZHANG³

¹College of Pipeline and Civil Engineering, China University of Petroleum (East China), Qingdao 266580, China

²West Pipeline Company of Pipe China, Urumqi 830013, China

³Sinopec Tianjin Liquefied Natural Gas Company Limited, Tianjin 300450, China
e-mail: zhoupeng_1998@163.com

MS received 16 October 2023; revised 23 December 2023; accepted 4 February 2024

Abstract. The excavation and maintenance of buried natural gas pipelines can lead to deformation and stress redistribution of the pipelines and even cause secondary damage to the pipes with issues. To clarify the impact of excavation unloading on buried pipelines, this study established a finite element three-dimensional pipe-soil model, investigated the mechanical response of pipelines under layered excavation and evaluated various parameters impacting the response. The parameters analyzed include the diameter-thickness ratio of the pipe, excavation length and width, thickness of top covering soil, elastic modulus of soil, specific weight of soil and initial displacement of the pipeline. The study results showed that the pipeline bulges upwards during excavation unloading, the pipe top in the middle is under tension, and the bottom of the pipe is under compression. Therefore, the axial stress and vertical displacement both increase first and then decrease, and they are distributed symmetrically along the pipeline axis; excavating the initially compressed pipeline leads to high strain areas in the pipeline and even local buckling. The response to slope excavation is more pronounced than that to straight trench excavation; the additional response of the pipeline increases with the increase of diameter-thickness ratio, excavation width, thickness of pipe top covering soil and specific weight of soil, but it decreases with the increasing soil elastic modulus. The additional response is closely related to excavation length and the initial displacement. The results of this study can provide a reference for pipeline construction, maintenance, and safety assessment.

Keywords. Excavation unloading; buried pipeline; numerical analysis; axial stress; vertical displacement; parameter analysis.

1. Introduction

Pipelines are inevitably experiencing issues such as cracking and corrosion over time during their service lifespan due to the impacts of the pipeline materials, construction technologies and working environments. These issues can adversely affect production safety. In recent years, excavation, inspection and repair works at vulnerable points of pipelines in harsh environments have been performed to take measures such as reinforcement, replacement, etc. according to different situations [1]. Excavating the soil above a pipe can alter the initial stress state of the soil, causing soil displacement around the pipe. Such displacement can result in the stress redistribution and deformation of the pipeline, and in severe cases, may lead to pipeline leakage or local damage.

Therefore, studying the mechanical response of buried pipelines under excavation unloading and evaluating the pipeline safety are of great significance.

Numerous scholars have investigated the impact of excavation unloading on tunnels or pipelines from three aspects: theoretical derivation, numerical simulation, and actual measurement. The two main methods used in the theoretical derivation are the two-stage method of additional load and two-stage method of additional displacement [2]. In the first stage, the vertical additional load and soil displacement generated by the excavation unloading in the axial direction of the pipeline were calculated respectively without considering the existence of buried pipelines. In the second stage, the deformation expression for the pipe is derived by considering the buried pipeline as an elastic foundation beam and applying load or displacement on it. Most scholars treated the tunnel as either a Timoshenko beam or an Euler–Bernoulli

*For correspondence
Published online: 04 April 2024

beam on the foundation [3] based on the Winkler foundation model [4–6], the Pasternak foundation model [7, 8], the Pasternak visco-elastic foundation model [9] and the Kerr foundation model [10–12]; thus, considering the unloading effect of the pit bottom and pit wall caused by foundation pit excavation, the tunnel deformation and internal force expressions are solved. Yao *et al* [13] analyzed the deformation of underground tunnels and pipelines based on the principle of the residual stress method combined with the layered springback summation method. Zhang *et al* [14] believed that the two-stage method of additional displacement should be adopted for tunnel excavation, while the two-stage method of additional load should be used for foundation pit excavation.

Regarding numerical simulation, many scholars have utilized finite element software such as ABAQUS [15–18] and FLAC3D [19] to create two-dimensional [20] and three-dimensional [21, 22] numerical models. They analyzed the mechanical response of the tunnel during excavation and studied the sensitivity of various parameters. Additionally, they proposed a simplified method for estimating tunnel deformation and internal force. Some scholars have considered the influence of excavation machinery on pipeline [23, 24]. In terms of actual measurement and analysis [25–28], researchers have summarized the overall law and time-space effect law of tunnel longitudinal deformation under foundation pit excavation through analyzing on-site monitoring data and also derived an empirical calculation method.

In summary, scholars have studied the responses of existing tunnels surrounding foundation pit projects in the unloading processes. In their analysis, they treated the foundation pit and the tunnel as independent structures. Nevertheless, the maintenance of buried natural gas pipelines typically requires excavating below the pipeline, and the excavation usually does not have the support as strong as foundation pit engineering. Therefore, the working conditions of buried pipelines and the tunnels is different. This paper established a finite element three-dimensional pipe-soil model, studied the mechanical response of buried pipelines under layered excavation and investigated impacts of various parameters related to pipe, soil and excavation on the response as shown in figure 1. The results of this study can serve as a reference for pipeline construction, maintenance, and safety evaluation.

2. Analytical model of pipeline under excavation unloading

2.1 Additional pipeline vertical stress caused by excavation

This paper aimed to study the effect of shallow excavation under the condition that there is no support or weak support on the pit wall. Therefore, only the vertical unloading effect

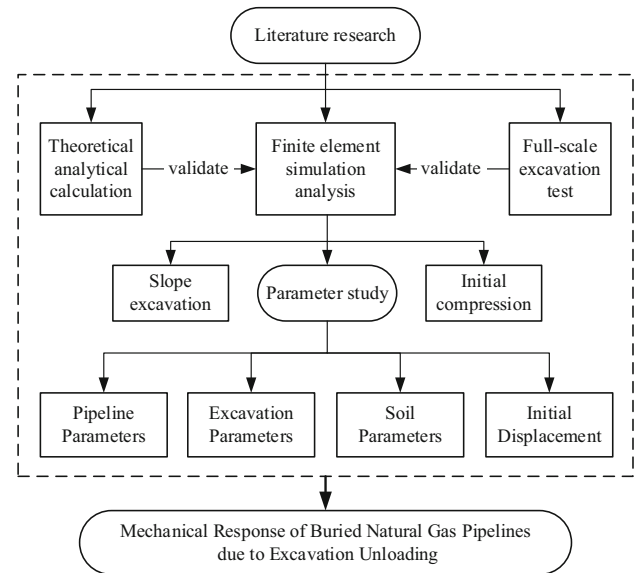


Figure 1. Pipeline response study flowchart.

at the bottom of the pit ($p = \gamma s$) was analyzed, and the integral of the basic solution of Mindlin [29] was used to solve the vertical additional stress. Figure 2 illustrates the theoretical model in the calculation [6].

In the figure, z_0 is the distance from the soil surface to the central axis of the pipeline; d is the pipe diameter; l is excavation length; b is excavation width; s is excavation depth. The center of the trench aligns with the center of the pipe; there is thus no angle between the two axes.

The point on the soil surface corresponding to the center of the trench is defined as the origin O of the coordinate system, and the coordinate directions are illustrated in figure 2. σ_z is the vertical additional stress at the point $(0, y, z_0)$ on the pipeline axis, which was generated under the action of unit force $p d \zeta d \eta$ at a bottom point of the trench (ζ, η, s) .

$$\sigma_z = \frac{\gamma s}{8\pi(1 - \mu_s)} \left\{ \begin{aligned} & (1 - 2\mu_s)(z_0 - s) \iint_{\Omega} \frac{d\zeta d\eta}{R_1^3} + 3(z_0 - s)^3 \iint_{\Omega} \frac{d\zeta d\eta}{R_1^5} \\ & - (1 - 2\mu_s)(z_0 - s) \iint_{\Omega} \frac{d\zeta d\eta}{R_2^3} \\ & + [3(3 - 4\mu_s)z_0(z_0 + s)^2 - 3s(z_0 + s)(5z_0 - s)] \iint_{\Omega} \frac{d\zeta d\eta}{R_2^5} \\ & + 30s z_0 (z_0 + s)^3 \iint_{\Omega} \frac{d\zeta d\eta}{R_2^7} \end{aligned} \right\} \quad (1)$$

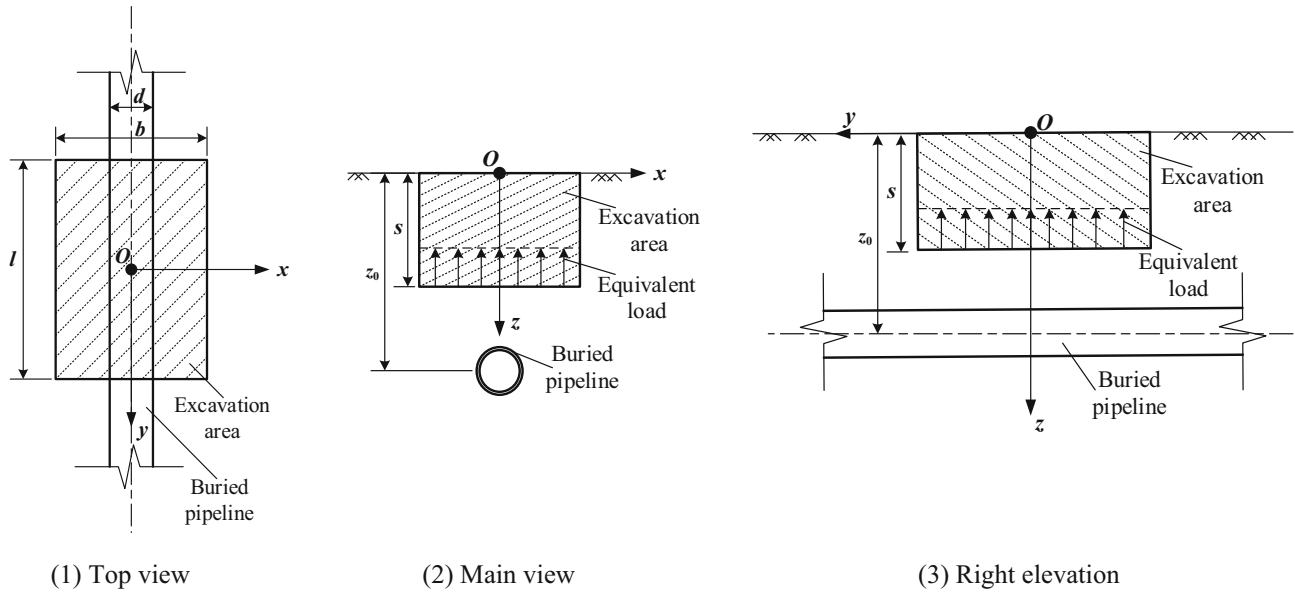


Figure 2. Calculation model of the effect of excavation unloading on pipeline.

$$\begin{cases} R_1 = \sqrt{\zeta^2 + (y - \eta)^2 + (z_0 - s)^2} \\ R_2 = \sqrt{\zeta^2 + (y - \eta)^2 + (z_0 + s)^2} \end{cases} \quad (2)$$

Where, Ω is the integral area of the trench, $-b/2 \leq \zeta \leq b/2$, $-l/2 \leq \eta \leq l/2$; μ_s is the Poisson's ratio of the soil.

Under the action of excavation unloading, the additional vertical load of the buried pipe at any point is

$$P_z(y) = \sigma_z d \quad (3)$$

2.2 Analytical solution of longitudinal pipeline deformation on Winkler foundation

The elastic foundation beam model is usually used to analyze the mechanical response of buried pipelines under additional loads. In this paper, buried pipelines are considered as infinitely long beams on double-sided Winkler foundations [30], as shown in figure 3. The pipeline maintains elastic contact with the surrounding soil, and the interaction is represented by a continuously distributed spring layer, satisfying the deformation coordination condition. Therefore, the mechanical differential equation of the buried pipeline under excavation unloading is expressed as

$$E_p I \frac{d^4 w(y)}{dy^4} + 2Kw(y) = P_z(y) \quad (4)$$

Where, E_p is the elastic modulus of the pipeline; I is the moment of inertia of the pipeline section; $w(y)$ is the vertical displacement of the pipeline, which is equal to the vertical displacement of the spring layer; $K = kd$, k is the

coefficient of the foundation bed [12], $k = E_s/D$; E_s is the elastic modulus of the foundation soil; D is the thickness of the foundation.

Equation (4) can be transformed into the stiffness matrix equilibrium differential equation using the finite difference method as follows:

$$\{K\} \cdot \{W\} = \{P\} \quad (5)$$

Where, $\{K\}$ is the stiffness matrix in the double-sided Winkler elastic foundation beam theory; $\{W\}$ is the pipeline displacement; $\{P\}$ is the additional load on the pipe.

The vertical displacement of the pipeline is obtained by solving Eq. (5).

3. Numerical analysis of effect of excavation unloading on pipelines

3.1 Experimental verification

To better investigate the impact of excavation unloading on pipelines, this study built an outdoor full-scale test station.

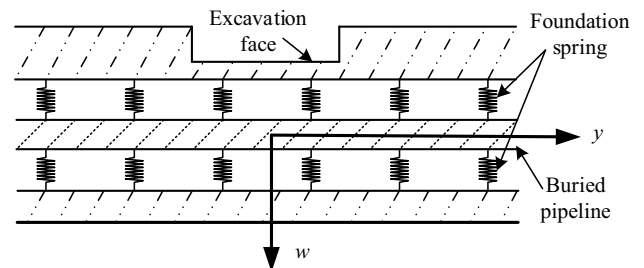


Figure 3. Schematic diagram of double-sided Winkler foundation.

The axial stress of the pipe top under the condition of excavation unloading was measured, and a corresponding three-dimensional finite element model was established. Figure 4 shows the comparison between the results from the experiment and the simulation. In the figure, the dimensions of the model are 24 m × 10 m × 8 m; the size of the excavation is 4 m × 2 m, and the height of each layer in the 2-layer excavation is 0.4 m; the size of the pipe is 1016 mm × 20 mm; the thickness of the pipe top covering soil is 0.9 m.

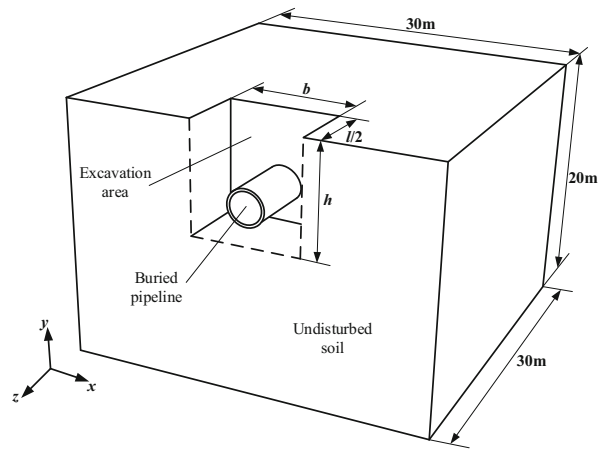
As shown in figure 4, both the simulated and measured top additional axial stresses exhibit a similar trend, featuring an upward convex distribution with high values at the middle and low values at both ends. The measured values of the first layer excavation are smaller than the simulated values, and the difference is big. This is because the surface soil in the experiment became denser after a long period of settlement, leading to an increase of the elastic modulus; however, this change of elastic modulus was not considered in the simulation. The measured values for the second excavation closely match the simulated values. Therefore, the simulation results can accurately demonstrate the mechanical response of pipelines to excavation unloading, which validates the reliability of the finite element model.

3.2 Finite element model

It can only be simplified to the plane strain problem [17] when the excavation length along the axial direction of the pipe is greater than 9 times the final excavation depth; hence, in this study, 3D finite element analysis is conducted by ABAQUS. Considering the boundary effect of the model, the excavation influence width is about 3 to 5 times

of the excavation depth, and the influence depth is about 2 to 4 times of the excavation depth [19]. In this paper, the model size is 60 m × 30 m × 20 m; the excavation length $l = 10$ m, and the width $b = 3$ m; the soil body is excavated in six layers, $h = h_1 + h_2 + h_3 + h_4 + h_5 + h_6 = 4.5$ m, as shown in figure 5.

In this paper, the research object is a X60 pipe with diameter $d = 1016$ mm, wall thickness $t = 20$ mm, density $\rho_p = 7850$ kg/m³, elastic modulus $E_p = 210$ GPa, Poisson's ratio $\mu_p = 0.3$, and yield stress $\sigma_y = 418$ MPa. The thickness of the pipe top covering soil is 3 m. The pipe is located at the center of the model and is parallel to the side of the model, and the internal pressure within the pipe is 8 MPa. The undisturbed soil is assumed as a uniform, continuous and isotropic Molar Coulomb material with density $\rho_s = 2000$ kg/m³, elastic modulus $E_s = 10$ MPa, Poisson's ratio $\mu_s = 0.3$, internal friction angle $\varphi = 25^\circ$, expansion



(1) Schematic diagram of finite element

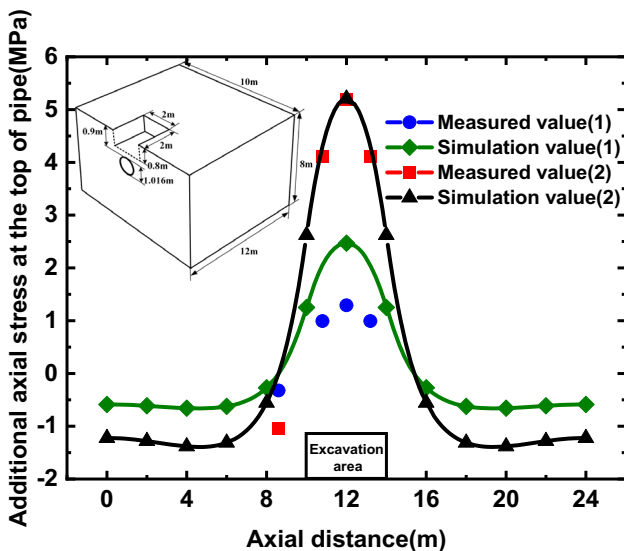
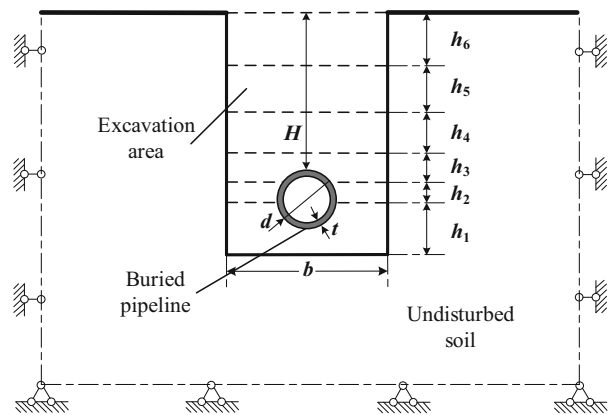


Figure 4. Comparison of experimental data and simulated data.



(2) Schematic diagram of the center section

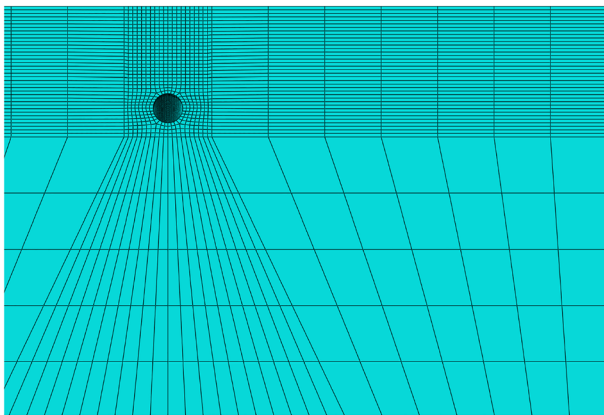
Figure 5. Schematic diagram of a 3D finite element model.

angle [19] $\psi = 0$, and cohesion $c = 20$ kPa. The interaction between the pipe and soil was simulated by setting surface-surface contact pairs, defining the coefficient of friction [31] between the contact surfaces as 0.315, and allowing the pipe and soil to separate after contact.

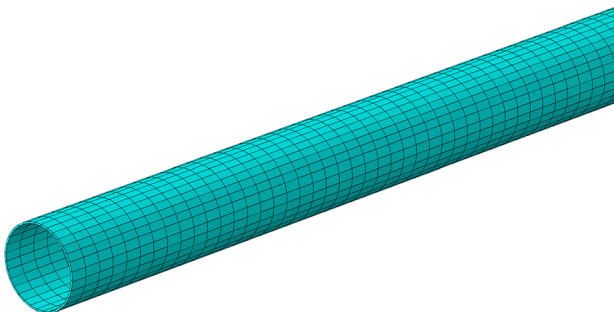
In the simulation, gravity and pipeline internal pressure were applied to the model. Once the soil stress was balanced, layered soil excavation was simulated through the life-death unit technology. The pipe and soil were meshed using eight-node linear hexahedral elements, and the grid around the pipe was refined. Figure 6 depicts the model meshing diagram. Horizontal constraints were applied around the model, and horizontal and vertical constraints were applied at the bottom.

3.3 Analysis of simulation results

The pipeline is subjected to additional load after excavation unloading. To demonstrate this phenomenon, figure 7 shows the stress and displacement response of the pipe during layered excavation. The in-situ stress balance process is denoted by Gb in this study, and the order of the excavation layer is denoted by E- i ($i = 1, 2, 3, \dots$).



(1) Schematic diagram of soil grids



(2) Schematic diagram of pipe grids

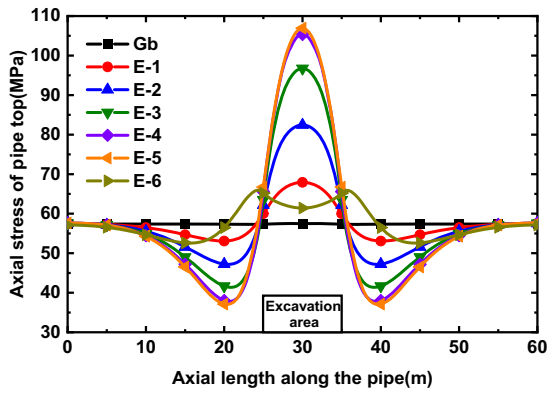
Figure 6. Model mesh schematic diagram.

As shown in figure 7, the entire pipe is in an axial tensile state before excavation, and the axial stress is approximately 57 MPa. Once unloading from excavation occurs above the pipe, the pipe rises upward, and additional axial tensile stress is generated at the top of the pipe in the excavation area, while additional axial compressive stress is generated at the bottom of the pipe. The axial stress of the pipe distributes symmetrically. The axial stress at the top of the pipe first decreases and then increases from the end of the pipe to the middle of the pipe, showing a W-shaped distribution. On the other hand, the axial stress at the bottom of the pipe first increases and then decreases, showing an M-shaped distribution. During excavating from the first layer to the fifth layer, the axial stress of the top of the pipe in the excavation area gradually increases to reach the maximum stress of 106.86 MPa, while the axial stress at the bottom of the pipe gradually decreases to the minimum stress of 8.58 MPa. When the sixth layer of soil is excavated, the pipe is completely exposed and suspended, the stress level is returned toward the initial state. The stress is distributed in a saddle shape along the axial direction of the pipeline. At the middle of the pipe, the stress at the top is 61.43 MPa and 52.21 MPa at the bottom, and the pipe stress concentrates at the edge of the trench.

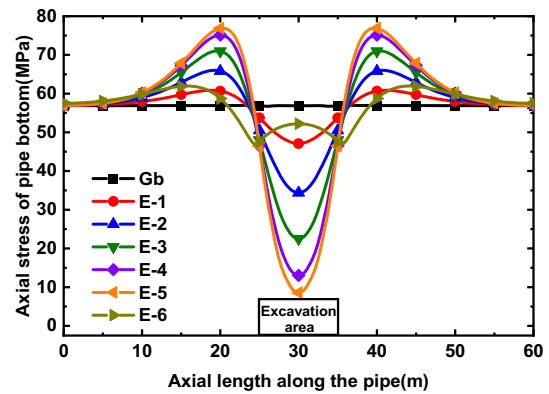
The vertical displacement of the pipe is approximately normally distributed along the axial direction of the pipeline, and gradually increases from the end of the pipe to the middle of the pipe. In the excavation process, the vertical displacement of the pipe first increases and then decreases, and the maximum displacement at the top is 18.37 mm and the bottom is 16 mm. When the sixth layer of soil is excavated, the pipe in the excavation area is completely exposed and suspended, losing the support of soil; thus, the pipe falls back, and the pipe section is flattened horizontally. The maximum vertical pipe displacement at the top is 5.52 mm, and 6.11 mm at the bottom.

After the parameters of Winkler's foundation model are calculated using the simplified elastic space method [12, 32], by substituting these parameters into Eq. (5), the theoretical vertical pipe displacement values at E-1 and E-2 can be obtained. As shown in figure 7(6), the theoretical calculation results and the numerical simulation results agree well, which once again proves that the numerical model in this paper is reasonable. When the excavation depth gradually deepens and the bottom of the trench approaches the pipeline, the calculation accuracy of the theoretical method is decreasing; therefore, using the finite element simulation method is necessary to study the mechanical response of the pipeline under excavation unloading.

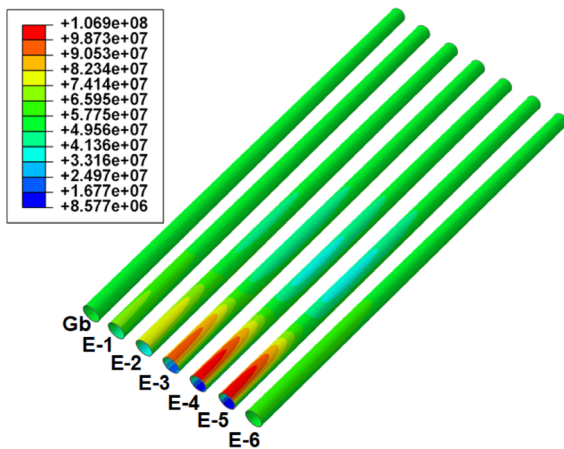
As shown in figure 7, the most noticeable response to the action of excavation unloading is at the middle of the pipeline, and the changes of stress and displacement at the top of the pipe tends to be more concerning than those at the bottom of the pipe. Therefore, this paper concentrates solely on analyzing additional stress and displacement at



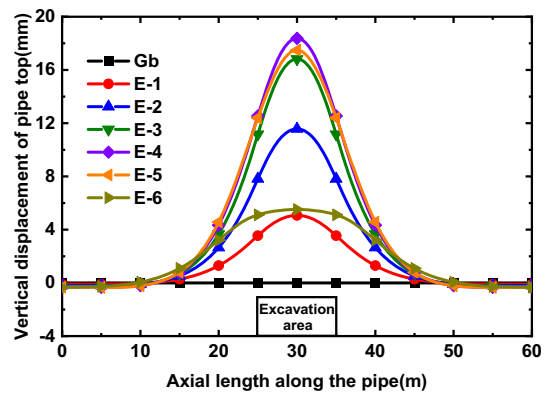
(1) Axial stress distribution at the pipe top



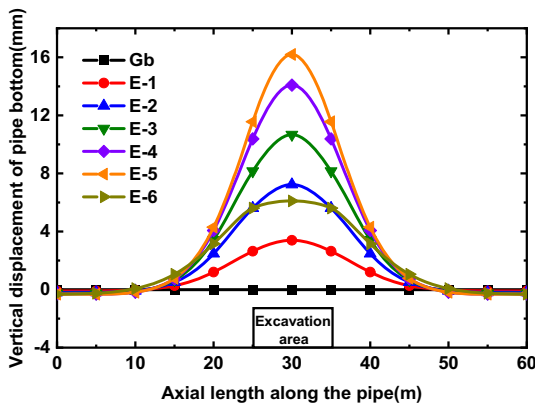
(2) Axial stress distribution at the pipe bottom



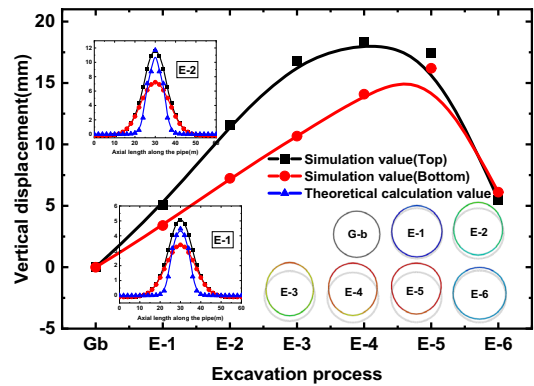
(3) Axial stress distributions in excavation process



(4) Vertical displacement distribution at pipe top



(5) Vertical displacement distribution at pipe bottom



(6) Vertical displacement in excavation process

Figure 7. Stress and displacement responses to excavation unloading.

the top of the pipe in the center section of the pipeline that are affected by various parameters of pipeline, soil and excavation.

Excavation unloading can cause local pressure at the bottom of the pipeline that is initially compressed, leading

to a high stress area. This can even result in buckling and crushing of the local section.

Figure 8 demonstrates that the initial axial pressure of the pipeline is 400 MPa, and plastic strain occurs at the pipe bottom in the middle of the pipeline and at the pipe top on both sides of the trench during the excavation process due

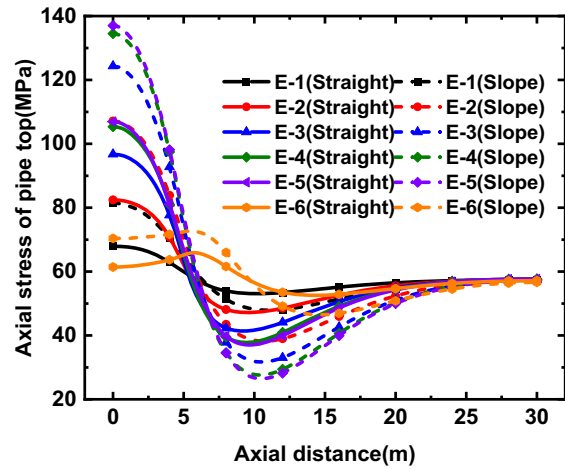
to the combined action of external pressure and soil unloading. After the excavation is completed, the deformation parameter of the central section of the pipeline is $\Delta = 3.18\%$, and the basic functions of the pipeline can still be maintained, but the passage of the internal detector is affected [33]. When the external pressure acting on the pipeline reaches a certain value, excavation can cause the collapse and buckling of the local pipeline. In severe cases, this may lead to the self-contact collision of the pipe inner wall, resulting in instability and damage of the pipeline.

Figure 9 shows the stress and displacement responses of the pipe top under 1:1 slope excavation and straight trench excavation. It can be seen from figure that the response of the pipeline during slope excavation is similar to that of straight trench excavation, but with a higher response amplitude. Moreover, the maximum axial stress at the top of the middle pipe increases by 28%, the maximum vertical displacement increases by 74%; the final axial stress increases by 15%, and the final vertical displacement increases by 146%. Therefore, without support, unloading response of the pipeline caused by slope excavation is more hazardous than by straight trench excavation.

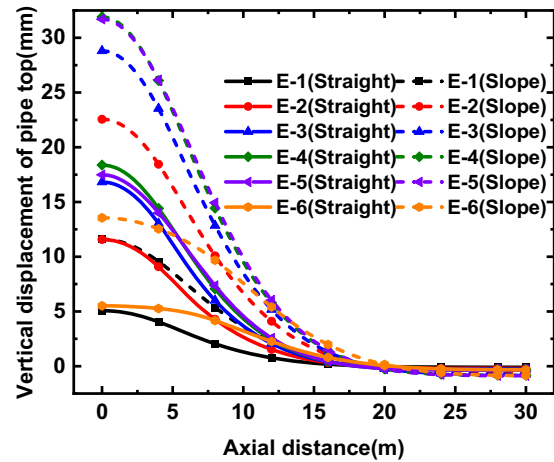
4. Effect of pipeline parameters on pipe response to excavation unloading

4.1 Diameter-to-thickness ratio

Figure 10 depicts the effect of the diameter-thickness ratio on the unloading response of the pipeline. In the analysis, the pipe diameter is 1016 mm, but the wall thickness are 26 mm ($d/t = 39$), 22 mm ($d/t = 46$), 20 mm ($d/t = 51$), 18 mm ($d/t = 56$), and 14.6 mm ($d/t = 70$), respectively, and other parameters remain unchanged.



(1) Axial stress distribution at the pipe top



(2) Vertical displacement distribution of pipe top

Figure 9. Comparison of pipeline response between slope excavation and straight trench excavation.

As shown in figure 10, with the increase of the diameter-thickness ratio, the final axial stress of the pipe gradually increases, and the high stress zone expands along the axial direction of the pipe and gradually approaches the center of the pipe. Both the maximum additional axial stress (vertical displacement) during excavation and the final additional axial stress (vertical displacement) after excavation gradually increase with the increase of the diameter-thickness ratio. When $d/t = 70$, compared to $d/t = 39$, the maximum and final additional axial stress on the pipe top increase by 13.17 MPa and 2.12 MPa respectively, and the maximum and final additional vertical displacement increase by 2.27 mm and 1.27 mm, respectively. The unloading response of thin-walled pipes is the most obvious, and damage is more likely to occur under the same working conditions.

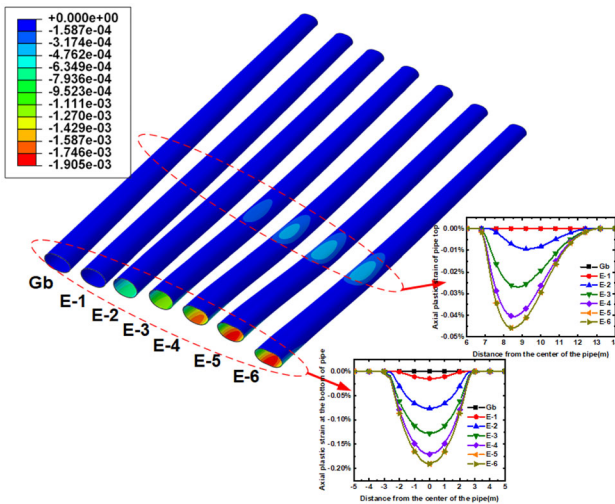
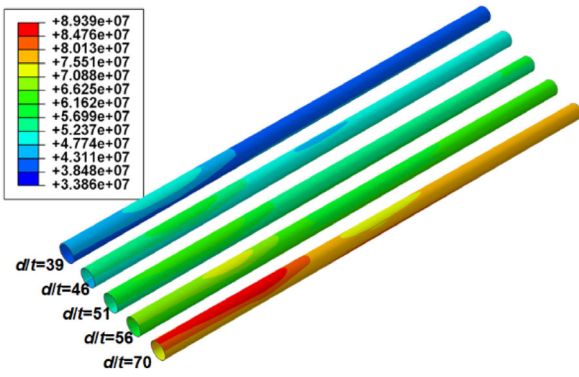
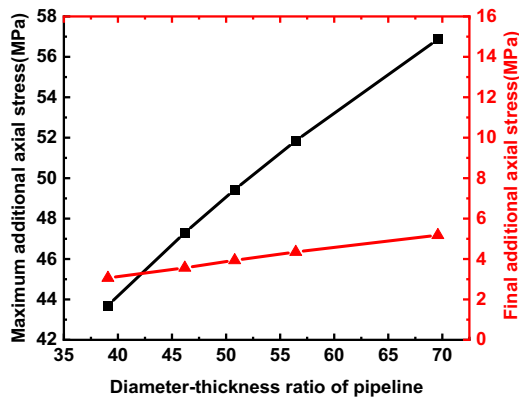


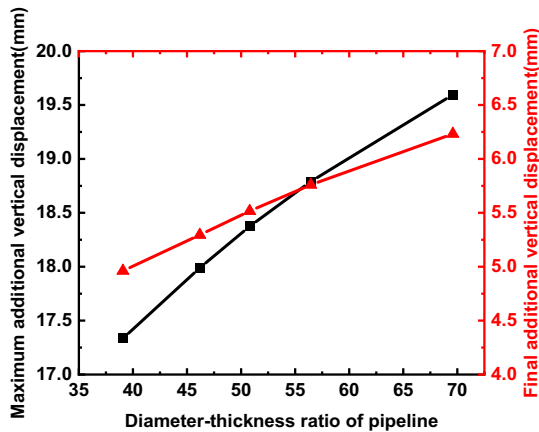
Figure 8. Distributions of deformation and plastic strain of the pressurized pipe in the excavation process.



(1) Cloud diagram of final axial stress



(2) Axial stress distribution at the pipe top



(3) Vertical displacement distribution of pipe top

Figure 10. Effect of diameter-to-thickness ratio on pipeline unloading response.

4.2 Thickness of pipe top covering soil

This study considers excavation beneath the pipeline; thus, the thickness of the pipe top covering soil determines the excavation depth of the pipeline. Figure 11 illustrates the impact of thickness of pipe top covering soil on the pipe

unloading response. The thickness was set to 1 m, 2 m, 3 m, 4 m, and 5 m, respectively, while other parameters remain unchanged.

According to figure 11, with the increase of the thickness of the pipe top covering soil, the final axial stress of the pipe gradually increases, and the high stress area expands along the axial direction of the pipe and gradually approaches the center of the pipe, thus causing the axial stress in the center of the pipe to gradually increase. Both the maximum additional axial stress (vertical displacement) during excavation and the final additional axial stress (vertical displacement) after excavation gradually increase with the thickness of the pipe top covering. Compared to the values at $H = 1$ m, at $H = 5$ m, the maximum and final additional axial stresses at the pipe top increase by 56.45 MP and 4.69 MPa, respectively, while the maximum and final additional vertical displacement increase by 21.22 mm and 4.71 mm, respectively. Hence, the thickness of the soil covering the pipeline has a significant impact on the unloading response of the pipeline. When excavating a deep-buried pipeline, it is necessary to provide proper support and closely monitor the response of the pipeline.

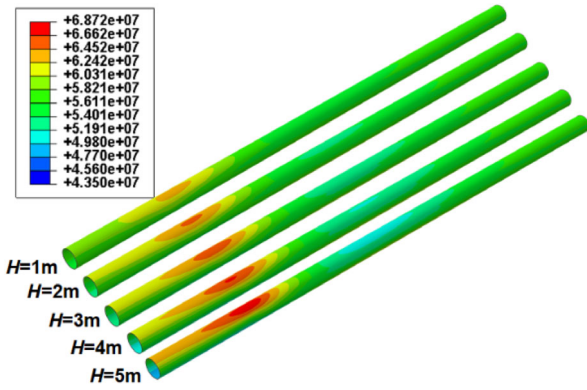
5. Effect of excavation parameters on pipe response to unloading

5.1 Excavation length

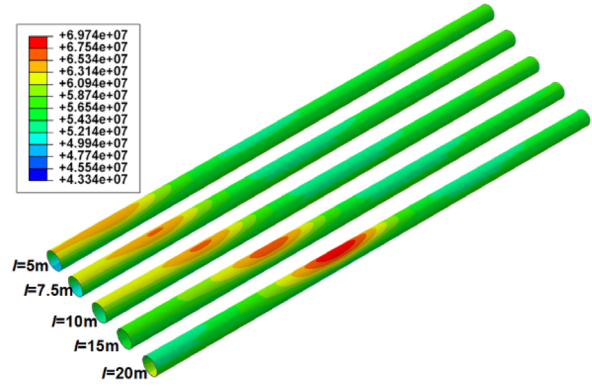
The excavation size directly impacts the unloading capacity at the bottom of the trench pit, thus affecting the unloading response of the pipeline. Figure 12 shows the effect of excavation length on the pipe unloading response. In the figure, the excavation length is 5 m, 7.5 m, 10 m, 15 m, and 20 m, respectively, and other parameters remain unchanged.

As shown in figure 12(1), as the excavation length increases, the final axial stress of the pipe gradually increases, and the high stress zone moves along the axial direction of the pipeline and gradually shifts away from the center of the pipeline. Consequently, the axial stress at the center of the pipeline gradually decreases.

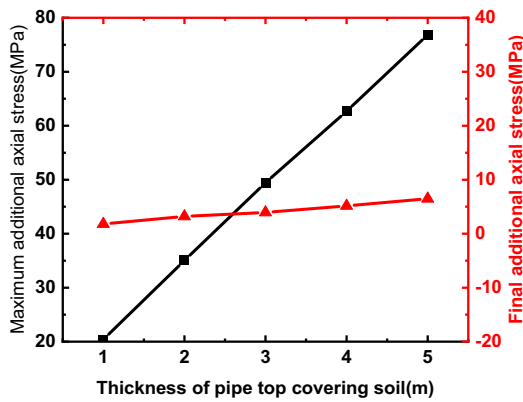
According to figure 12, the maximum additional axial stress and the final additional vertical displacement under excavation unloading initially increase and then decrease with the increase of excavation length. At $l = 10$ m, they reach their maximum values of 49.43 MPa and 5.52 mm, respectively. The final additional axial stress gradually decreases while the maximum additional vertical displacement of the pipeline gradually increases. Therefore, when excavating the pipeline under the working conditions of this study, the excavation length greater than 10 m can be selected since the additional axial stress and the final additional vertical displacement of the pipeline will gradually decrease; however, it is critical to control the



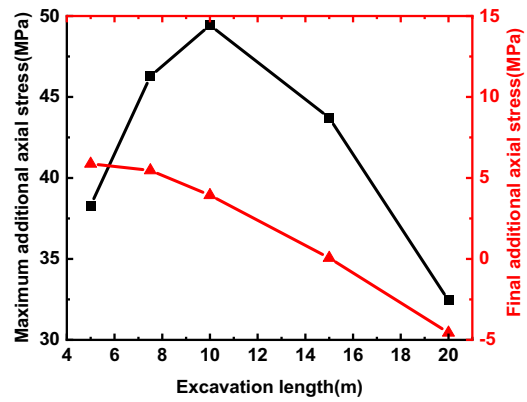
(1) Cloud diagram of final axial stress



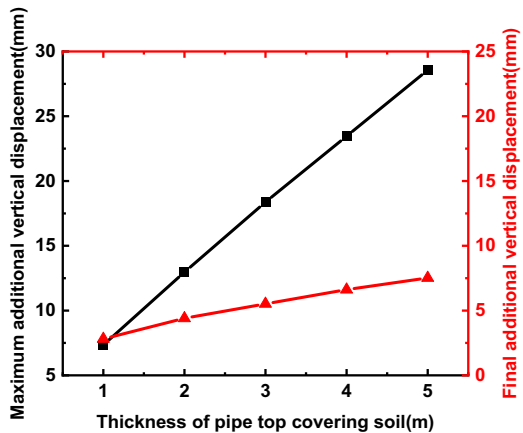
(1) Cloud diagram of final axial stress



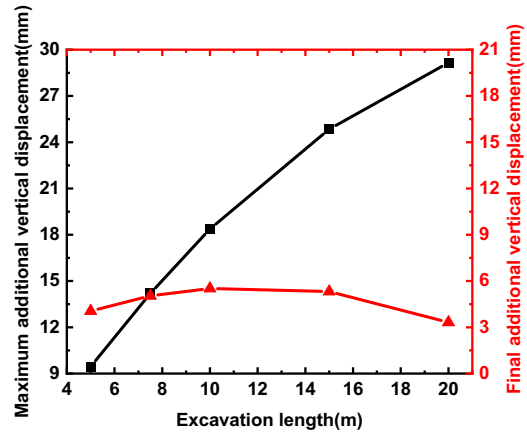
(2) Axial stress distribution at the pipe top



(2) Axial stress distribution at the pipe top



(3) Vertical displacement distribution of pipe top



(3) Vertical displacement distribution of pipe top

Figure 11. Effect of thickness of top covering soil on pipeline unloading response.

Figure 12. Effect of excavation length on pipeline unloading response.

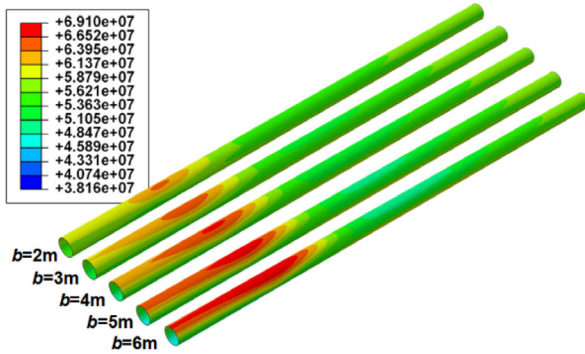
maximum additional vertical displacement during the excavation process.

5.2 Excavation width

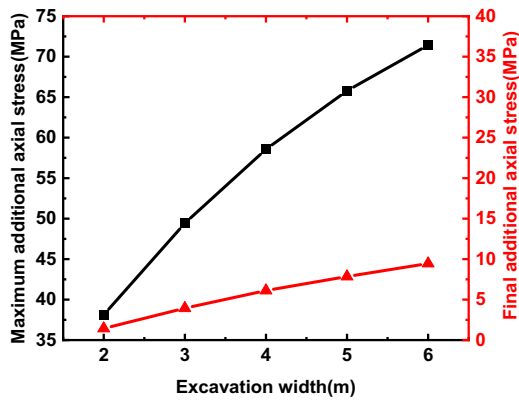
Figure 13 demonstrates the impact of excavation width on the pipe unloading response. In the figure, the excavation width is 2 m, 3 m, 4 m, 5 m, and 6 m, respectively, and other parameters remain unchanged.

As shown in figure, with the increase of excavation width, the final axial stress of the pipeline gradually increases, and the high stress zone expands along the axial direction of the pipeline to approach the center of the pipeline, resulting in the gradual increase of the axial stress in the center. The maximum additional axial stress (vertical displacement) during excavation and the final additional

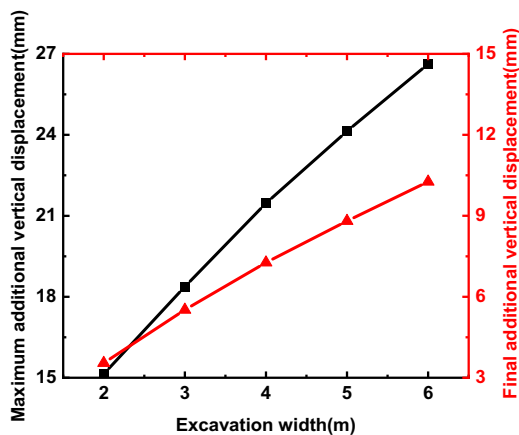
axial stress (vertical displacement) after excavation both gradually increase with increasing excavation width. Compared to the values at $b = 2$ m, At $b = 6$ m, the maximum and final additional axial stresses at the top of the pipe increase by 33.31 MPa and 8.02 MPa, respectively, and the maximum and final additional vertical displacement increase by 11.49 mm and 6.71 mm, respectively. Therefore, the excavation width should be controlled based on the actual demand during pipeline excavation in order to reduce the additional stress and displacement of the pipeline.



(1) Cloud diagram of final axial stress



(2) Axial stress distribution at the pipe top



(3) Vertical displacement distribution of pipe top

6. Effect of soil parameters on pipe response to excavation unloading

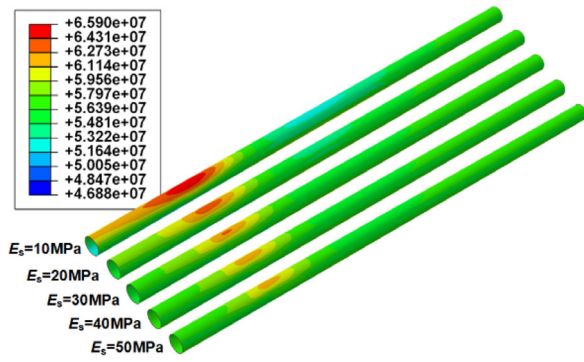
The soil surrounding the buried pipe is the medium between the trench and the pipeline. The load generated by excavation and unloading affects the pipeline through the soil, so the parameters of the soil surrounding the pipe are closely related to the unloading response of the buried pipeline.

6.1 Elastic modulus

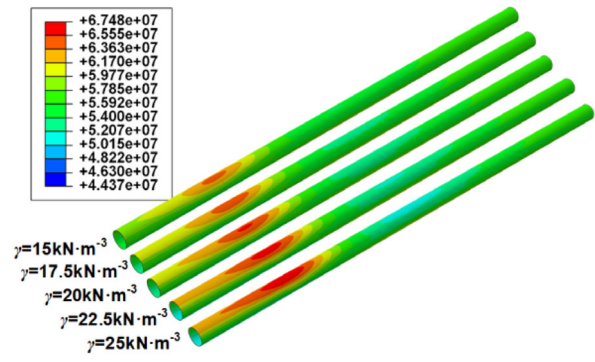
Figure 14 shows the impact of the elastic modulus of soil on the pipe unloading response. The elastic modulus was set to 10 MPa, 20 MPa, 30 MPa, 40 MPa, and 50 MPa, respectively, while other parameters remain unchanged.

As depicted in the figure, with the increase of the elastic modulus of the surrounding soil, the final axial stress of the pipeline gradually decreases, and the high stress zone decreases along the axial direction of the pipe and gradually moves away from the center, resulting in the gradual decrease of the axial stress at the center of the pipeline. Both the maximum additional axial stress (vertical displacement) during excavation and the final additional axial stress (vertical displacement) after excavation decrease with the increase of the elastic modulus. Compared to the values at $E_s = 10$ MPa, at $E_s = 50$ MPa, the maximum and final additional axial stresses at the pipe top reduce by 30.70 MPa and 4.48 MPa, respectively, and the maximum and final additional vertical displacement reduce by 13.23 mm and 4.63 mm, respectively. This is because when the elastic modulus of the soil surrounding the pipeline is small, the soil's ability to adjust to unloading is limited, and a larger proportion of the additional load is transmitted to the pipeline. Conversely, when the elastic modulus of the soil is large, the soil can better adjust to unloading, thereby reducing the unloading response of the pipeline.

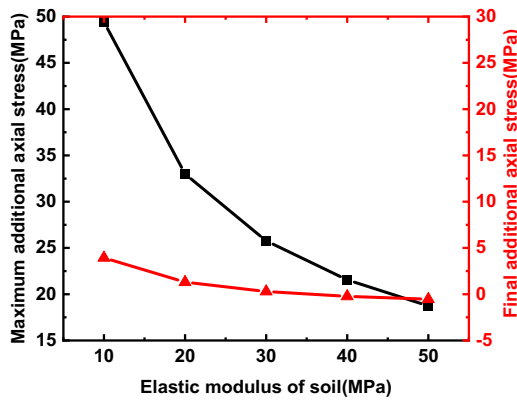
Figure 13. Effect of excavation width on pipeline unloading response.



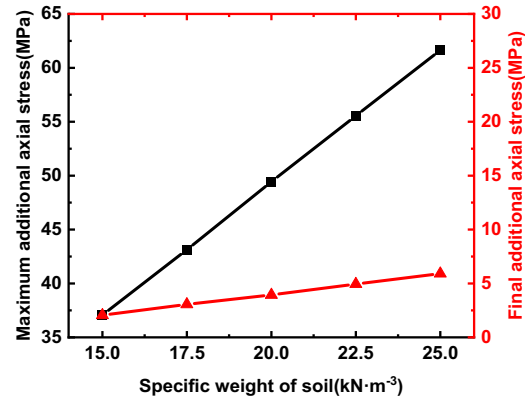
(1) Cloud diagram of final axial stress



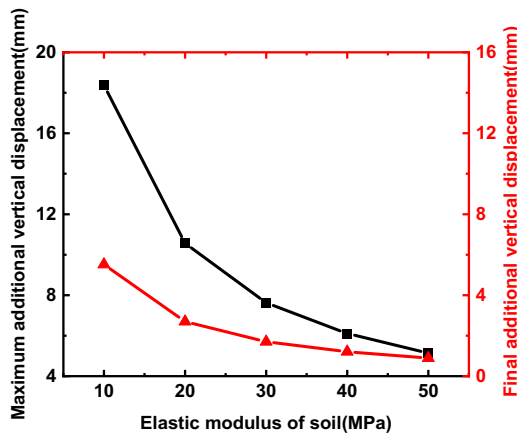
(1) Cloud diagram of final axial stress



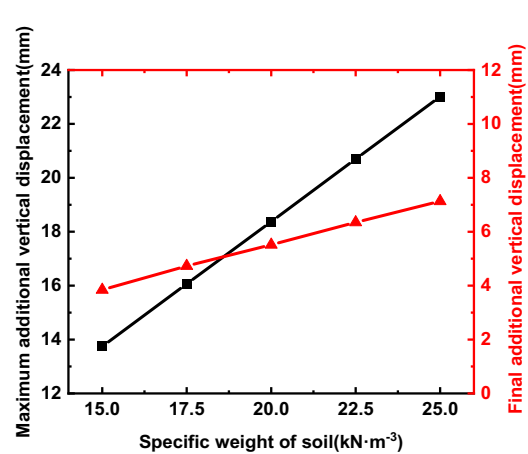
(2) Axial stress distribution at the pipe top



(2) Axial stress distribution at the pipe top



(3) Vertical displacement distribution of pipe top



(3) Vertical displacement distribution of pipe top

Figure 14. Effect of soil elastic modulus on pipeline unloading response.

Figure 15. Effect of specific weight of soil on pipeline unloading response.

6.2 Specific weight of soil

Figure 15 shows the impact of the specific weight of soil on the pipe unloading response. The specific weight of soil in the study was set to 15 kN·m⁻³, 17.5 kN·m⁻³, 20 kN·m⁻³, 22.5 kN·m⁻³, and 25 kN·m⁻³, respectively, while other parameters remain unchanged.

As shown in figure 15, with the increase of the specific weight of soil, the final axial stress of the pipe gradually increases, and the high stress area expands along the axial direction of the pipe and gradually approaches the center of the pipe, thus causing the axial stress in the center of the pipe to gradually increase. Both the maximum additional

axial stress (vertical displacement) during excavation and the final additional axial stress (vertical displacement) after excavation gradually increase with the specific weight of soil. Compared to the values at $\gamma = 15 \text{ kN}\cdot\text{m}^{-3}$, at $\gamma = 25 \text{ kN}\cdot\text{m}^{-3}$, the maximum and final additional axial stresses at the pipe top increase by 24.60 MPa and 3.86 MPa, respectively, while the maximum and final additional vertical displacement increase by 9.27 mm and 3.29 mm, respectively. Hence, the specific weight of soil has a significant impact on the unloading response of the pipeline. When the specific weight of soil is high, it is necessary to provide proper support and closely monitor the response of the pipeline.

7. Effect of initial displacement of pipe on bulging deformation

7.1 Shape of initial displacement

The causes of accidents in long-distance oil and gas pipelines mainly include mechanical damage, corrosion, manufacturing defects and natural disasters. Among them, mechanical damage, corrosion and manufacturing defects are mainly manifested as local damage to the pipeline body, while natural disasters cause additional deformation of the pipeline through the disturbance of the ground. In this

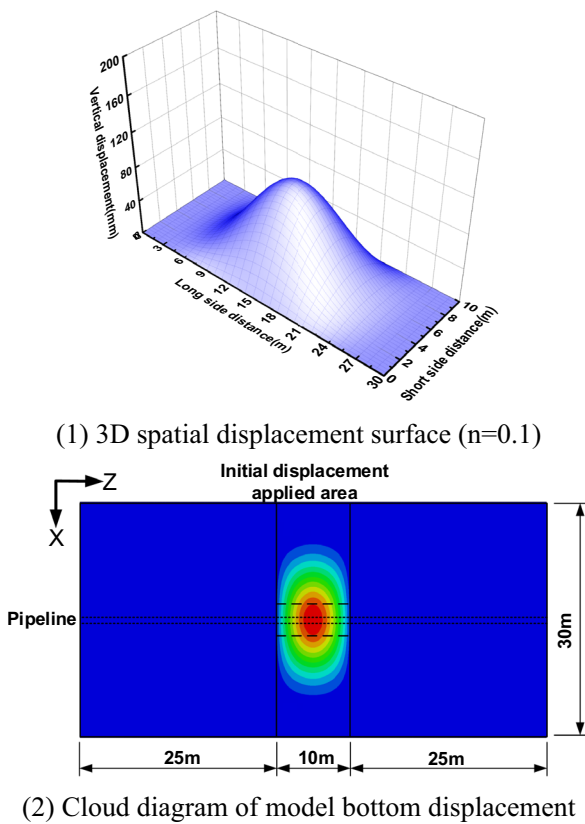
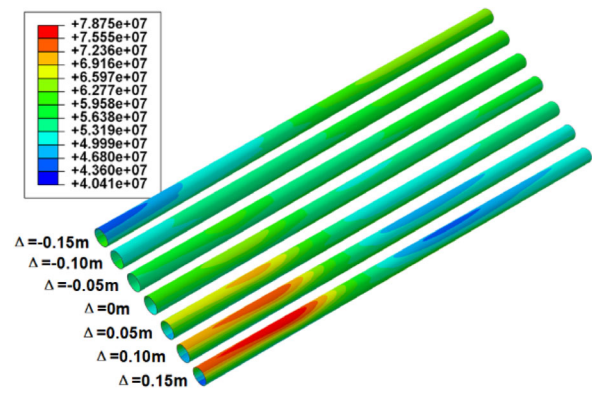
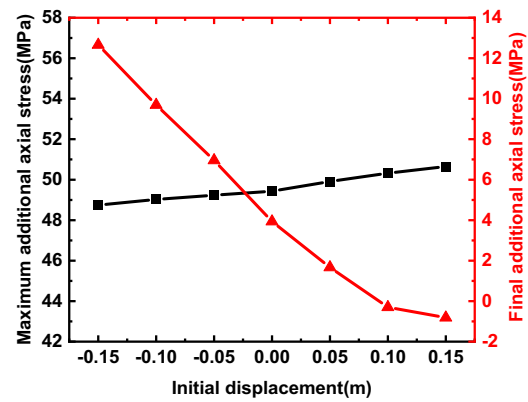


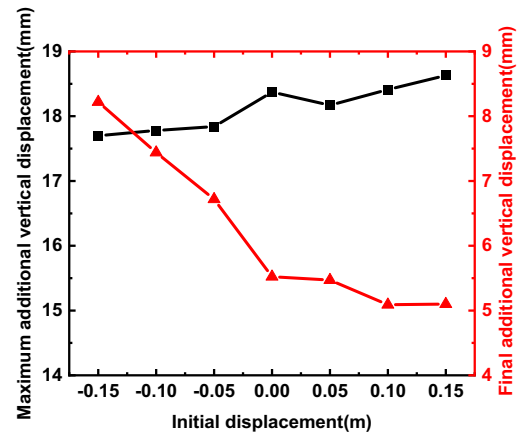
Figure 16. Initial applied displacement.



(1) Cloud diagram of final axial stress



(2) Axial stress distribution at the pipe top



(3) Vertical displacement distribution of pipe top

Figure 17. Effect of initial displacement on pipeline unloading response.

study, the initial vertical displacement was applied to the bottom of the model through the DISP subroutine in ABAQUS to simulate the initial deformation of the pipeline caused by natural disasters, as shown in figure 16.

The three-dimensional spatial displacement equation for the bottom of the model is

$$y = n \cdot \sin^4\left(\pi \frac{x}{30}\right) \cdot \sin\left(\pi \frac{z-25}{10}\right) \quad (6)$$

Where, n is any real number; $x \in [0, 30]$; $z \in [25, 35]$.

7.2 Impact of pipe initial displacement

Excavation unloading can cause the top of the pipe to be under axial tension and the bottom of the pipe to be under axial compression. When the initial displacement is downward ($n < 0$), the pipe bottom is under axial tension relative to the top of the pipe before excavation. This response is opposite to the excavation response; thus, the excavation process tends to make the pipe stress state safer. On the other hand, when the initial displacement is upward ($n > 0$), the pipe top is under tension relative to the pipe bottom before excavation, which is the same as the excavation response. As a result, the excavation process with upward initial displacement tends to make the stress state of the pipe more unsafe.

Figure 17 illustrates the effect of the initial vertical displacement of the pipe on the unloading response of the pipeline. The values of n was set to -0.15 , -0.10 , -0.05 , 0.00 , 0.05 , 0.10 and 0.15 , while other parameters remain unchanged.

As shown in figure 17, with the increase of the initial vertical displacement of the pipeline, the final axial stress of the pipeline gradually increases, and the pipe top in the excavation area transfers from a low-stress zone to a high-stress zone; moreover, the maximum additional axial stress (vertical displacement) during excavation increases slightly, while the final additional axial stress (vertical displacement) after the excavation gradually decreases. Compared to the values at $n = -0.15$, at $n = 0.15$, the maximum additional axial stress and vertical displacement at the pipe top increases by 1.90 MPa and 0.93 mm, respectively, while the final additional axial stress and vertical displacement decrease by 13.47 MPa and 3.12 mm, respectively. The initial displacement of the pipe has a relatively small effect on the maximum additional response of the pipeline, but it can have a significant impact on the final additional response of the pipeline.

8. Conclusion

(1) Under excavation unloading, the pipeline bulges upwards, the top of the middle pipe is under axial tension, and the bottom of the pipe is under axial compression; the stress and displacement are symmetrically distributed along the pipeline axis. The axial stress at the top of the pipe shows a W-shaped distribution while the axial stress at the bottom exhibits an M-shaped distribution. In addition, the vertical displacement is normally distributed. During the

excavation process, the axial stress and vertical displacement first increase and then decrease. When the pipeline in the excavation area is completely exposed and suspended, the pipeline partially falls back, the axial stress is distributed in a “saddle-shaped” along the axial direction of the pipeline, and the pipeline section is flattened horizontally.

- (2) When the pipeline is initially compressed, excavation unloading can cause a high stress zone at the bottom of the pipeline, resulting in a large compressive strain and even causing the buckling and crushing of the local pipe section.
- (3) Under the condition of no support, the response law of the pipeline under slope excavation is the same as that of the straight trench excavation, but the amplitude of the response to unloading due to the slope excavation is greater. The maximum axial stress of the pipe top and the final axial stress increased by 28% and 15%, respectively; the maximum vertical displacement and the final vertical displacement increased by 74% and 146%, respectively.
- (4) Parameter sensitivity law of pipeline unloading response is summarized as follows:
 - a. The additional axial stress and vertical displacement of buried pipelines gradually increase with the diameter thickness ratio, excavation width, thickness of pipe top covering soil and specific weight of soil, and gradually decrease with the increase of soil elastic modulus.
 - b. The maximum additional axial stress and the final additional vertical displacement both initially increase and then decrease with the increase of excavation length; eventually, the additional axial stress gradually decreases, while the maximum additional vertical displacement gradually increases.
 - c. The initial displacement of the pipe has little effect on the maximum additional response but has a greater impact on the final additional response.
- (5) However, it is worth noting that the parameter studies carried out in this paper do not show the significance of each parameter. At the same time, it is urgent to establish a theoretical analytical model for the response of natural gas pipeline under such excavation conditions, so as to guide the practical project.

References

- [1] Xian G D and Lyu Y 2020 Inspection and disposal of girth weld defects of oil and gas pipelines. *Petroleum Tubular Goods & Instruments* 6(02): 42–45
- [2] Jiang Z 2014 Theoretical analysis on deformation of pipeline caused by adjacent foundation pit excavation. *Chinese*

- Journal of Underground Space and Engineering* 10(02): 362–368
- [3] Zong X 2016 Study of longitudinal deformation of existing tunnel due to above excavation unloading. *Rock and Soil Mechanics* 37(S2): 571–577+596
- [4] Biot M A 1937 Bending of an infinite beam on an elastic foundation. *Journal of Applied Mechanics* 59: 1–7
- [5] Vesic A B 1961 Bending of beams resting on isotropic elastic solids. *Journal of Engineering Mechanics* 87(2): 35–53
- [6] Zhang Z G, Zhang M X and Wang W D 2011 Two-stage method for analyzing effects on adjacent metro tunnels due to foundation pit excavation. *Rock and Soil Mechanics* 32(07): 2085–2092
- [7] Zhao W, Liang Y H, Jiang J and Xing X W 2022 Analysis of uplift deformation of the longitudinal obliquely passing metro tunnel caused by excavation of foundation pit. *Science Technology and Engineering* 22(09): 3688–3695
- [8] Zhou Z L, Chen S G, Tu P and Zhang H S 2015 An analytic study on the deflection of subway tunnel due to adjacent excavation of foundation pit. *Journal of Modern Transportation* 23(004): 287–297
- [9] Zhou Z L, Chen S G, Chen L and Tu P 2015 Analysis of uplift deflection of subway tunnel due to adjacent pit excavation. *Chinese Journal of Geotechnical Engineering* 37(12): 2224–2234
- [10] Kerr A D 1965 A study of a new foundation model. *Acta Mechanica* 1(2): 135–147
- [11] Avramidis I E and Morfidis K 2006 Bending of beams on three-parameter elastic foundation. *International Journal of Solids and Structures* 43: 357–375
- [12] Huang X, Huang H W and Zhang D M 2012 Longitudinal deflection of existing shield tunnels due to deep excavation. *Chinese Journal of Geotechnical Engineering* 34(07): 1241–1249
- [13] Yao Y M, Yang J G and Wang Z 2013 Analysis on influence of the foundation pit excavation on the deformation of subjacent tunnels and pipelines. *Chinese Journal of Underground Space and Engineering* 9(S2): 2029–2033
- [14] Zhang Z, Zhang M and Zhao Q 2015 A simplified analysis for deformation behavior of buried pipelines considering disturbance effects of underground excavation in soft clays. *Arabian Journal of Geosciences* 8(10): 7771–7785
- [15] Zheng G and Wei S W 2008 Numerical analyses of influence of overlying pit excavation on existing tunnels. *Journal of Central South University of Technology* 15(S2): 69–75
- [16] Shi J, Ng C and Chen Y 2015 Three-dimensional numerical parametric study of the influence of basement excavation on existing tunnel. *Computers and Geotechnics* 63(jan.): 146–158
- [17] Shi J, Ng C and Chen Y 2017 A simplified method to estimate three-dimensional tunnel responses to basement excavation. *Tunnelling and Underground Space Technology* 62(feb.): 53–63
- [18] Wu Z, Yao L F, Chen X L, Zhang H Z and Xu C J 2021 Numerical analysis on the influence of the foundation pit excavation on the vertical deformation of subjacent pipelines. *Science Technology and Engineering* 21(07): 2843–2849
- [19] Du J L and Yang M 2009 Influence analysis of excavation of deep pit on adjacent buried pipelines. *Chinese Journal of Rock Mechanics and Engineering* 28(S1): 3015–3020
- [20] Dolezalova M 2001 Tunnel complex unloaded by a deep excavation. *Computers & Geotechnics* 28(3): 469–493
- [21] Chen R P, Meng F Y, Li Z C, Ye Y H and Ye J N 2016 Investigation of response of metro tunnels due to adjacent large excavation and protective measures in soft soils. *Tunnelling & Underground Space Technology* 58: 224–235
- [22] Zhang J, Xie R and Zhang H 2018 Mechanical response analysis of the buried pipeline due to adjacent foundation pit excavation. *Tunnelling and Underground Space Technology* 78: 135–145
- [23] Yao A L, Xu T L, Zeng X G and Jiang H Y 2015 Numerical analyses of the stress and limiting load for buried gas pipelines under excavation machine impact. *Journal of Pipeline Systems Engineering & Practice* 6(3): A4014003
- [24] Xu D, Chen L Q, Yu C, Zhang S, Zhao X and Lai X 2023 Failure analysis and control of natural gas pipelines under excavation impact based on machine learning scheme. *International Journal of Pressure Vessels and Piping* 201: 104870
- [25] Chen Y and Zhang D M 2004 Analysis of monitoring data on tunnel heaving due to unloading of foundation pit excavation. *Underground Space* 24(5): 748–751
- [26] Bi S Q, Gan B L, Liang Y H, Yang Y H, Li H, Cui H and Bian C 2022 Measurement and analysis of the influence of foundation pit excavation on existing short distance tunnel. *Science Technology and Engineering* 22(03): 1198–1204
- [27] Li Z G, Liu H, Liu G B and Bi H M 2005 Influence analysis of deep-dip excavation on down tunnel based on the measured displacement. *Chinese Journal of Underground Space and Engineering* 04: 619–623
- [28] Guo P F, Yang L C, Zhou S H, Gong Q M and Xiao J H 2016 Measurement data analyses of heave deformation of shield tunnels due to overlying pit excavation. *Science Rock and Soil Mechanics* 37(S2): 613–621
- [29] Mindlin R D 1936 Force at a point in the interior of a semi-infinite solid. *Physics* 7(1): 195–202
- [30] Xu W D and Jiang J 2018 Calculation formula for longitudinal deformation of adjacent metro tunnel due to foundation pit excavation. *Railway Engineering* 28(09): 63–67
- [31] Vazouras P, Karamanos S A and Dakoulas P 2010 Finite element analysis of buried steel pipelines under strike-slip fault displacements. *Soil Dynamics and Earthquake Engineering* 30(11): 1361–1376
- [32] Kerr A D 1985 On the determination of foundation model parameters. *Journal of Geotechnical Engineering* 111(11): 1334–1340
- [33] Yu Y, Li Z M, Yu J X, Sun W Z, Liu X W, Ma J D and Liu C 2022 Buckling failure analysis of subsea buried pipeline crossing strike-slip fault. *Engineering Mechanics* 39(09): 242–256
- Springer Nature or its licensor (e.g. a society or other partner) holds exclusive rights to this article under a publishing agreement with the author(s) or other rightsholder(s); author self-archiving of the accepted manuscript version of this article is solely governed by the terms of such publishing agreement and applicable law.